JPL PUBLICATION 78-73

Alleviation of Pressure Pulse Effects for Trains Entering Tunnels - Final Report

Volume I: Summary

Bain Dayman, Jr., et al

June 1979

Prepared for
U.S. Department of Transportation
Urban Mass Transportation Administration
Through an agreement with
National Aeronautics and Space Administration
by
Jet Propulsion Laboratory
California Institute of Technology
Pasadena, California

The research described in this publication was carried out by the Jet Propulsion Laboratory, California Institute of Technology, and was sponsored by the Department of Transportation through an agreement with NASA.

JPL PUBLICATION 78-73

Alleviation of Pressure Pulse Effects for Trains Entering Tunnels - Final Report

Volume I: Summary

Bain Dayman, Jr. (JPL)
Andrew G. Hammitt (Consultant)
Harold P. Holway (JPL)
Curtis E. Tucker, Jr. (JPL)
Alan E. Vardy (Consultant)

June 1979

Prepared for
U.S. Department of Transportation
Urban Mass Transportation Administration
Through an agreement with
National Aeronautics and Space Administration
by
Jet Propulsion Laboratory
California Institute of Technology
Pasadena, California

ABSTRACT

This study on Tunnel Entry Pressure Transits (TEPT) was carried out for the Transportation Systems Center of the U.S. Department of Transportation in order to determine to what degree it is possible to attenuate the effects of pressure pulses on the passengers in trains entering tunnels. The emphasis of this study is on the approach of modifying the normally abrupt portal of a constant-diameter single-track tunnel.

In order to understand this approach, it was first necessary to have an analytical model in which confidence exists in its capability to predict realistic pressure pulse histories of trains entering tunnels having porous and/or flared tunnel portals. To accomplish this, available theoretical information along with small-scale laboratory experiments were used to update an existing computer program. Good comparisons were obtained of the subsequent analytical model experiments carried out in a one percent scale facility. Then, the computer program was used to develop several examples of effective portal configurations.

Although the suggested modifications to the tunnel entrance portal may not appreciably decrease the magnitude of the pressure rise, they are very effective in reducing the discomfort to the human ear by substantially decreasing the rate of pressure rise to that which the normal ear can accommodate. Qualitative comparison was made of this portal modification approach with other approaches: decreasing the train speed or sealing the cars. The optimum approach, which is dependent upon the conditions and requirements of each particular rail system, is likely to be the portal modification one for a rapid rail mass transit system.

FOREWORD

The results of this study have been published by the Department of Transportation (DOT) as "Alleviation of Pressure Pulse Effects for Trains Entering Tunnels," Final Report, UMTA-MA-06-0100-79-10, June 1979 as a single volume. However, this rather large report contains only a small portion of the large amount of data accumulated during this study. Therefore, JPL decided to publish two additional volumes, I and III. This Volume I presents a summary of the study, as well as a summary of Volume III, "Supplemental Experimental Data." JPL has incorporated the DOT report as Volume II of its three volume presentation of the study results. Volume III presents all of the raw data to permit subsequent analysis and must be requested directly from the first author. In order to properly utilize Volume III, it will be necessary to refer to Volume II which can be obtained directly from the National Technical Service (Springfield, VA 22161).

It should be noted that the report published by DOT has no reference to the existence and availability of companion reports (Volumes I and III of the JPL reports). Also, there is no reference in the DOT report to the JPL Publication 78-73.

The purpose of Volume I is to give a brief summary of the study results. Rather than prepare a special report, use was made of the papers presented by two of the authors at the Third International Symposium on the "Aerodynamics and Ventilation of Vehicle Tunnels," sponsored by BHRA Fluid Engineering, held at Sheffield University, Sheffield, England, on 12-21 March 1979. These papers are included here just as they were presented: the first, on the "Experimental Program," Paper H2, was presented by Bain Dayman, Jr.; the second, on "Theoretical Modelling and Experimental Correlation," Paper H3, was presented by Alan E. Vardy. For convenience, Volume II and Volume III Tables of Contents are included in this volume as an Appendix.

PAGE IV INTENTIONALLY BLANK

TABLE OF CONTENTS

ALLEVIATION OF TUNNEL ENTRY PRESSURE TRANSIENTS: 1. EXPERIMENTAL PROGRAM

Bain Dayman, Jr., B.Sc., M.Sc., P

Jet Propulsion Laboratory, California Institute of Technology, Pasadena, California, U.S.A.

And

Alan E. Vardy, B.Sc., Ph.D., C.Eng., M.I.C.E.

University Engineering Department, Cambridge, U.K.

SUMMARY

When a train enters a tunnel, pressure pulses occur which may cause passenger discomfort. The usual approaches to this problem are: let the riders suffer some auditory discomfort; restrict the train speed; or, in some cases, use sealed cars. The Transportation Systems Center, with funding from the Urban Mass Transportation Administration, both of the U.S. Department of Transportation, initiated this study in an endeavor to evaluate aerodynamic approaches for coping with this problem. The primary objective was to compare analytical predictions with experimental results. In order to have appropriate experimental results for comparison purposes, it was necessary to set up a simple small-scale laboratory facility and run a series of tests.

This paper describes in detail the experimental program that was carried out. An inexpensive laboratory facility of one percent scale was constructed and equipped with pressure transducers. Model trains were launched into a tube at speeds up to 30 m/s by a slingshot-type device. Several types of entrance portals were used: unventilated constant diameter; ventilated (the porosity was up to 1% of the wall surface area); and flared (the upstream end was 2½ times the tube area). Also, tests were run with a vent shaft near the entrance. On occasions, the exit end was restricted with various sizes of orifices. The data from this experimental program was used primarily to validate the analytical model. However, the data can be used to obtain a quantitative understanding of the various effects of tunnel and train geometries upon the pressure transients along a tunnel generated by a train entering a tunnel.

At the conclusion of the experimental and theoretical phases of this study, a brief cost study was performed in order to determine if tunnel entrance portal extensions are economically feasible. It was shown that they can be for urban subway systems.

1. INTRODUCTION

1.1 Rationale for Experimental Program

Adequate experimental information is not available for developing and validating the existing theories and analytical approaches such as those by Fox and Henson[1], Vardy[2], Barrows[3], and Yamamoto[4]. The full-scale information on actual trains was obtained for relatively uncontrolled conditions. Experimental information on perforated portals does not exist. Therefore, it was necessary to conduct experiments in order to obtain the required data.

The cost effectiveness of small-scale tests appeared very attractive. Since the pressure transient information that was needed to verify theory is relatively independent of viscosity, a facility as small as one percent of the actual situation was considered to be satisfactory. Therefore, that scale was selected for the experimental program to simulate a 2000 m long tunnel.

1.2 Facility

The facility consisted of four primary elements: model launcher; tube (including entry/exit portals and a vent shaft); train models; instrumentation (including pressure ports). Figure 1 is a schematic of the basic facility while Figure 2 is a photograph of the actual 1% scale facility.

1.2.1 Model Launcher

The launcherwas a simple folded slingshot using three fabric-coated rubber bungie cords (see Figure 3). The bungie cords were connected to a sabot which in turn pushed against the base of the model. Launch speed was adjusted by decreasing the initial length and/or tension of the bungie cords. The launcher was cocked by an electric motor pulling on the back of the sabot. The total travel of the sabot was about 1.5 m. It was able to launch a 0.25 kg model at speeds up to 30 m/s. The model (with tri-skids fore and aft) was guided to the tube entrance by three circumferentially-located, equally-spaced tracks.

A pair of photocells was used to determine real-time velocity of the model when entering the tube (see Figure 3a). The oscilloscope data is necessary to obtain accurate model speeds; the significant pressure transient events are excellent indications of the model speed along the tube. The models were "caught" in a padded box located one meter beyond the tube exit.

1.2.2 Tube

1.2.2.1 Basic Tube

The basic tube is 5.04 cm I.D. and is in three 6½ m lengths that were bolted together by the use of flanges (Figures 1 and 2). The interior walls were honed smooth. The entrance end of the tube had an additional flange located at the vent-shaft position. This 2 m length of tube was removable in order to facilitate the incorporation of various entry portals.

1.2.2.2 Entry Portals

The perforated portals were made by drilling holes along the end portions of the tube. For the most part, the holes were equally spaced around the tube circumference at 90° intervals. The 3 mm D holes in the 6½ mm thick tube wall did not simulate the expected full-scale situation where the hole diameter

would be in the order of 20-30 cm in a portal wall thickness of 10-20cm. However, the use of appropriate orifice coefficients will properly account for this geometric difference.

The porosity is defined as the total area of all of the holes in the perforated length ratioed to the cross-section area of the inside of the tube. All desired hole patterns existed simultaneously in the 2 m length used for the perforated entry portal. Any holes not desired were simply taped over (see Figures 2 and 3b). The effect of this approach was checked for the zero porosity case: all holes taped over vs a tube having no holes whatsoever; no effect was apparent.

The flared entry portal was limited to one configuration. It was conical, 1 m long, and had an entrance area that was nominally 2½ times the tube area (see Figure 4). The tri-tracks decreased this nominal area ratio to 2.1 at flare entrance

When a perforated exit portal was used, it was identical to the entry one. In addition to the portal "extensions", simple orifices which restricted the flow at the tube ends were used to alter the characteristics of the reflected waves.

1.2.2.3 Vent Shaft

A 15 cm long, 5 cm I.D. vent-shaft was located about 2 m from the tube entrance. Normally, it was sealed off flush to the tube I.D. It could be opened fully to its 5 cm I.D., or have orifices located either at the upper end or the tube-wall end. Also, its I.D. could be decreased along its entire length. A picture of it is shown in Figure 5.

1.2.3 Train Models

The trains were represented by aluminum tubes which were sealed off at each end with the corners slightly rounded (see Figure 6). Skids were located at both ends of the models which rode along the tri-guides of the launcher and centered the models in the tube. The diameters of the 55 cm long train models were varied to obtain blockage ratios of 25%, 50%, and 75%. The effect of train length was determined by including a 110 cm long version of the 50% blockage model.

1.2.4 Instrumentation

The tube-wall pressures at each of the measuring stations (Figure 1) were generally recorded with a pair of transducers. Statham diaphragm-type (upper-trace) gave an accurate overall magnitude of pressure while Kistler piezo-electric-type (lower trace) gave a more accurate indication of rapid pressure change than the Stathams (due to their longer response time and ringing). Unfortunately, these Kistler transducers could not record a constant pressure level over 5 ms in time without a considerable drop-off in the recorded measurement. Nevertheless, with the above considerations taken into account, the accuracies are within 5%. The last station (1372) far down the tube had only a Kistler transducer. Figure 7 shows the typical data obtained.

The quality of the pressure data was considerably improved toward the end of the test program when a Kulite transducer was obtained. It was specifically matched for the pressure range expected, had rapid response time and could make absolute measurements. An example of the data for this tranducer (which was located at Station 225) is in Figure 8. For one run, a Kulite transducer was installed at Station 25. Numerous other transducer changes were made during the program. Also, it should be noted that stations are measured from the tube entrance. To accomplish this, it was necessary to move some transducers for the few runs when the tube was shortened at the entrance end.

Provision was made for a considerable number of ports to which pressure transducers could be attached. A typical arrangement is shown in Figure 2. A single port was located at Stations 1372 and 1272; double ports at Stations 125, 325, 425; eight ports, used for calibration purposes, were at Station 225. Again, double ports were at Stations 825 and 525 which were used for the diaphragm-burst runs. For Run 203, two pressure transducers were located at Station 25 in order to observe the development of the pressure pulse close to the open end of the perforated entry portal.

It would have been desirable to obtain pressure data on the side of the model as it entered and traveled along the tube. In this way, a direct measurement would be made of the pressure pulses that the passengers inside a train would experience. Limited effort was expended to accomplish this using the Kulite transducer. Although some encouraging results were obtained, the quality was not up to that of the measurements along the tube wall. Therefore, it was decided that the use of the analytical model would yield a better comparison of the characteristics of the tube-wall and train-wall pressure pulses than direct experimental measurements.

1.3 Test Procedures

1.3.1 Calibrations

One example of each of the three types of pressure transducers used was independently calibrated with an oil manometer. Both static and dynamic calibrations were performed. Because of the nature of the piezoelectric transducers, they could not be statically calibrated. The dynamic calibration was generated by suddenly opening to atmosphere the pressurized line at the transducer. The response of the transducers to a step change in pressure was inititally determined in this manner. The comparisons between the static and dynamic calibrations were quite good.

"In situ" dynamic calibrations were performed on all of the transducers by mounting them all at the same station on the tube (225) and then launching a model into the tube having a normal entry portal. The step wave with a nearly level plateau was ideal for both comparing the response characteristics and for determining the appropriate relative calibration factor of each transducer. The dynamic calibrations showed that the high-pressure range piezoelectric transducers that were used were not sufficiently stable at pressure to maintain a pressure reading for even as short a time as 5 ms. That is why the diaphragm type transducers were used even though these had poor time response. An example of a calibration run is shown in Figure 9.

The time scales on the oscilloscopes were calibrated by observing the occurence of a characteristic wave as it progressed at the speed of sound along the tube. All of the calibrations were conducted several times during the course of the experimental program. The accuracies are within 3%.

1.3.2 Testing

1.3.2.1 Model-Train Runs

Pressure histories at four stations along the tube were obtained for virtually every run. A wide variety of conditions were investigated in the experimental program, much more than necessary to achieve the objectives of this study. Simulation of critical features such as the vent shaft, various portal geometries, model speed, length and blockage was necessary in order to put the validation of the analytical model to a true test. The effort and time required to perform additional variations were relatively small, so nearly an order of magnitude of additional runs was made. A good portion of the conditions investigated is listed in Table 1. A complete index of runs is in Reference 5.

1.3.2 Diaphragm - Burst Runs

A series of runs were made by bursting a diaphragm that sent a controlled pressure pulse down the tube in order to investigate wave reflection from the tube end. The downstream portion of the tube was sealed, pumped up to a fixed pressure of 1.05 or 1.10 atmospheres. Then the milar diaphragm was ruptured by heating a nichrome wire which encircled it. An example of this type of data appears in Figure 10. Since the repeatibility was not as ideal as that for the model runs, many repeat runs were made. None of this data has been analyzed.

1.3.3 Data Reduction

Only enough runs were reduced in order to determine the capability of the analytical model to predict the pressure histories along the tube. The scale factors for all oscilloscope traces were obtained from the previously discussed calibration procedures. As the many remaining runs which have not been analyzed at all would be useful in carrying out a detailed analysis of the wide spectrum of experimental results, they are made available by including all of the oscilloscope traces in Reference 5.

2. ANALYSIS OF DATA

2.1 Train Parameters

The influence of the train lengths is well illustrated by the runs with model lengths of 55 and 110 cm in which the tunnel is a simple parallel tube. The pressure traces in the two cases are built up of the same basic elements, but the resulting patterns exhibit considerable differences. The complete picture depends upon the superpositions of the waves and upon the times at which the nose and tail of the train pass the transducers.

The effect of blockage ratio with the basic configuration is important. The shapes of the pressure histories are very similar to one another, but the pressure magnitudes are highly sensitive to the blockage ratio. In particular, the nose-entry wavefront varies approximately in the ratio 1:2:8 for blockage ratios of 25%, 50% and 75%. The tail-entry wavefront will vary similarly, but its importance is shown to be less because of attenuation in the annulus between the train model side and the tube wall.

For one run, the train sides were perforated in order to simulate leakage around doors, etc. on full-scale trains (Figure 6). This had negligible effect on the flow structure in the tunnel. This is because only small quantities of air are required to change the air pressures inside the vehicle. For the leakage to significantly influence the tunnel airflows, it would be necessary for the axial velocities through the train to attain high values, thus reducing the effective blockage area of the vehicle.

Several runs were made with an enlarged diameter of the vehicle tail. A gradual build-up produces a much more clearly defined pressure history at each transducer than an abrupt build-up. This is convenient for the purposes of analysis, but it is less desirable in a full-scale circumstance. It would be possible to completely eliminate the tail-entry wavefront (except for three-dimensional effects) by using slightly smaller build-ups than were tested. This would be highly desirable because passengers close to the rear of the train are subjected to the full magnitude of this wavefront even though those at the front benefit from the subsequent attenuation in the annulus.

2.2 Tunnel Parameters

2.2.1 Perforated Entry

The most extensively investigated tunnel modification in the experimental test program was the perforated entrance region. Various lengths of the perforated region and also a variety of wall porosities were tested.

The influence of the length of the perforated region was investigated for a porosity of 50% of the tunnel cross-sectional area. The characteristic shape and magnitude of the nose-entry wavefront is roughly independent of the length of the perforated entry, but the rate of change of pressure in the tunnel is approximately inversely proportional to the length. This is a highly desirable feature because it indicates that advantage can always be gained from longer regions even when these exceed the length of the train. In addition to the immediate advantages resulting from the reduced pressure gradients, there is a reduction in the magnitudes of some of the pressure fluctuations. This occurs whenever the elongated wavefronts overlap with themselves or with one-another as occurs when the tube is short enough and/or the train speed is low enough.

A less fortunate property of perforated entrance regions is also demonstrated, namely that the tail-entry wavefront is not elongated as much as the nose-entry wavefront. This difficulty could be overcome by building-up the tail of the train. Then the nose-entry effects would be alleviated by the perforated region, but the tail-entry effects would not require alleviation. It may be deduced that these two modifications can complement one another very well.

The optimum total porosity appears to be about 75% of the tunnel cross-sectional area. The pressure histories are not very sensitive to moderate changes in this value or to changes in the distribution of the porosity. This is fortunate because the optimum total value will depend upon such things as the skin friction in the annulus as well as the upon the train speed and blockage ratio.

2.2.2 Flared Entry

A natural alternative to a perforated entrance region is a flared entry portal. Both of these devices have much in common and their respective influences on the pressure histories are broadly similar. Nevertheless, important differences exist. The maximum pressure rise for the flared portal is less than for the perforated one. Also, the shapes of the pressure rises differ because of the different manners in which the two devices influence the tail-entry wavefront. It has already been shown that the influence of tail-entry is not felt downstream of a perforated region until the tail has almost reached the end of the region. In contrast, the flared entrance elongates this wavefront approximately as effectively as for the nose-entry wavefront. The fall in pressure due to tail-entry counter balances the rise due to nose-entry. Of course, this property will be less important when the train is longer than the entrance region. Even in that case reduced skin friction in the annular region as well as diffuser action of the flared entrance will lead to a smaller peak pressure than that found with a perforated entrance.

The flared entry portal in the experimental program did not act as an efficient diffuser, but this should not be taken as an absolute guide to the behaviour in a full-scale tunnel. Nevertheless, it is reasonable to suppose that little pressure recovery will occur at full-scale unless care is taken to provide a smooth joint between the tunnel and the flare. One run was made with a flared entrance portal which was slightly perforated. Since the porosity was small, the flare effect dominated, but there is evidence of a reduced elongation of the tail-entry wavefront. It would appear that there is little point in using the combined device.

2.2.3 Airshafts

The influence of airshafts has been well demonstrated.[2] Broadly speaking, they can reduce the effects of the entry transients, but only at the expense of creating additional sources of wave activity. A delicate balance must be maintained in which the size and position of the shafts are matched with the size and speed of the train. The restricted airshaft did provide very useful attenuation, but the short, large-bore shaft was of little help as the wavefronts generated at the shaft were almost as great as those generated by train-entry in the basic configuration.

2.2.4 Exit Restrictions

By blanking-off the tube exit except for a 1 cm diameter orifice, the reflection of the nose-entry wavefront was virtually eliminated. A simple explanation for its effectiveness is that a fully open end causes a total negative reflection whereas a fully closed end causes a total positive reflection. Intermediate openings cause intermediate reflections.

The blockage ratio at the exit can be chosen so that no reflection occurs when a design-wavefront of any stipulated magnitude reaches the orifice. Wavefronts of other magnitudes will reflect either positively or negatively depending upon whether they are of greater or smaller magnitude than the design-wavefront. Analysis of this phenomenon is straightforward.

There are important practical restraints on the design of suitable restrictions. For example, the 1 cm orifice was only 20% of the tube diameter. Such a restriction cannot be provided as a permanent rigid fixture in a real tunnel. Two alternatives exist. Either the blockage must be removed before the arrival of the vehicle, or the blockage must be in the form of a flexible device which the train can safely penetrate. Water curtains and air curtains have been suggested as possible restrictions because they can fit into either category, but they may have undesirable side effects.

The use of flow restrictions in tunnels is a topic which merits attention. Important advances could be made with such devices, especially if they are modulated by means of active controls which respond to air pressures or to the proximity of trains.

2.2.5 Example Results

At the end of the test program, a series of runs were made using the Kulite pressure transducer. Selected examples of the oscillograph traces are presented in Figure 11 to show the reader the effects of several test variables on the observed pressure transients. The test conditions and oscillograph scale information are in Table 3.

3. TRADE-OFF STUDY

The main purpose of the overall study was to assess the tunnel tailoring approach for alleviating the pressure pulse problems on the passengers of a train entering a tunnel. In addition, a brief comparison was made of the cost and service aspects for the various pressure pulse alleviation approaches in order to put them into the proper perspective.

The assumption was made that the rate of pressure rise inside the cars must be held to tolerable limits. For normal cars, the pressure pulse inside the car closely follows on the outside of the car. In an actual case, should it not be practical to adequately alleviate the pressure pulse using only a geometrically-tailored tunnel, it can be complemented by a partial speed-restriction approach. The direct and indirect costs of each approach are estimated. These estimates should suffice to demonstrate the important trade-off principles.

3.1 Requirements

The maximum rise of the pressure pulse inside the train is limited to 0.41 kPa (0.06 psi) (as per Carstens)[6] with a maximum rate of 0.34kPa/s (0.05 psi/s). This is shown in Figures 12 and 13 by the lines labeled "limit". From the computer results, it can be seen that an entry speed of 80 mph results in a pressure pulse which exceeds the suggested limits for passengers riding in a typical train. Restricting the entry speed to 60 mph (see Figure 12) decreases the entry pressure pulse to below the limit. The use of an extension to the entry portal can keep the entry pressure pulse that the passengers sense below the suggested limit. This is shown in Figure 13 using results from the computer model. Sketches of portal extensions are shown in Figure 14.

3.2 Comparison of Costs

The comparison of the costs of several approaches to the alleviation of the entry pressure transient is shown in Table 2. The "No Speed Restriction" case utilizes the 200 m long 50% porous constant-diameter portal extension. Information from References 7 and 8 were used to estimate the cost of the portal extension which came out to be around $180K.

There are two ways of restricting tunnel entry speed. The first is to limit station to tunnel speed at 60 mph; the increase in time is 11 seconds if there was just enough distance (about 4000 ft) for the train to have reached 80 mph prior to reaching the tunnel. The second is to allow train acceleration to 80 mph and then brake to 60 mph at the approach to the tunnel, then go back up to 80 mph inside the tunnel; this approach would result in a 5 sec increase in time. In order to make a rational cost comparison of the portal extension with the restricted speed approach, it is necessary to put some arbitrary value on the time increase. This was done assuming $5/hr for each of the 100 passengers per subway train (made up of 4 cars each) and is shown as "people".

Costing out the TE*at 5 cents per kwh and the BE*at half that, it is apparent that the yearly energy costs of the 80-60-80 mph approach exceed the effective yearly cost (10% of the total) of the portal extension. When the lost time of the passengers is considered, the total yearly costs (direct and indirect) of the restricted speed approaches significantly exceed the assumed yearly amortization cost of the 200-m long perforated portal extension (by a factor of about 5). A similar total yearly cost results for the 60 mph top speed between the station and the tunnel entrance; but in this case, it is due entirely to the assumed cost of lost time.

No estimate was made for the cost of sealing a subway car in order to sufficiently alleviate the pressure pulse that the passengers would sense. There are at least three factors in the design of the cars which must be considered: air leak through the many doors (can be as many as ten per car with eight of them being automatically operating); transmittal of the pulse through the ventilation and/or conditioning system; the pressure difference effect on the car structure. It should be noted that any pressure pulse problems that occur in the tunnel itself are unaffected. British Rail has estimated that the leak requirements must be below $0.003 m^2$ per car [9] (a more severe requirement than for commerical passenger airplanes). It is not at all clear that it is practical to meet these requirements for subway cars. In any case, it would be reasonable to expect a significant increase in the cost of a car in order to achieve the leak requirement, say on the order of $100 K per car.

No cost estimates of any kind were carried out for the initiation of flow in the tunnel approach. In an actual subway system, this can be done in two ways. The passive one is attractive as it has no costs associated with it at the times the frequency of trains is high. The only requirement is that there be at least another train in the tunnel traveling in the same direction. The piston action (where the induced air flow through the tunnel can easily be on the order of 25% of the train speed [10] was shown during the experimental program to be very effective in alleviating the pressure pulse everywhere in the tunnel.

Since most subway systems have powered ventilation systems (which are not all necessarily in operation) it is conceivable that they could be used to cause the desirable air flow in the tunnel. The cost may be reasonable. However, if special fan systems have to be incorporated in a subway system (and especially for adding to an existing system), the cost may be higher than for the portal extension.

Unless there are a great many tunnels and just a few train cars, it does not appear that the sealed-car approach can be competitive with the other approaches for subway train speeds up to 80 mph. For the train speeds of 120 mph, the costs of the other approaches will increase dramatically** while the sealed-car approach stays about the same (or possibly decreases since it would likely occur for an intercity passenger train which has a simpler door configuration than a subway train). Additional trade-off analysis is required for a high-speed intercity train in order to reach a conclusion on the best approach.

* TE is traction effort; BE is braking effort

** For example, the perforated portal extension would have to be lengthened from 200 m to 675 m in order to keep the nose entry pulse within limits.

REFERENCE

1. Fox, J.A. and Henson, D.A.: "The Prediction of the Magnitudes of Pressure Transients Generated by a Train Entering A Single Tunnel". Proc. of Civ. Engrs., 49, pp 53-69, May, 1971

2. Vardy, A.E., "The Use of Airshafts for the Alleviation of Pressure Transients in Railway Tunnels", Proceedings of the Second International Symposium on the Aerodynamics and Ventilation of Vehicle Tunnels, Organized by BHRA, Cambridge U.K., March 1976.

3. Barrows, T.M., "Tunnel Entry Pressure Transients", International Conference On Transportation, Los Angeles, California, July, 1976.

4. Yamamoto, A., "On the Gradual Pressure Rise by a Flared Tunnel Entrance", RTRI Quarterly Report (Japan) Vol. 6, No. 4, 1965.

5. Staff, "Experimental Data Obtained During the Study of the Alleviation of Pressure Pulse Effects for Trains Entering Tunnels", JPL Publication No. 78-73, August, 1978.

6. Carstens, J.P., "Literature Survey of Passenger Comfort Limitations of High Speed Ground Transportation", PB168 171, 1965.

7. Dayman, Bain, et al, "Alternative Concepts for Underground Rapid Transit Systems Vol.IIC, Supporting Studies - Capital Equipment", Report DOT-TST-77-31, IIC, March, 1977.

8. "Alternative Concepts for Tunnel Transit Systems" Cost Estimates of Mined Tunnels", A Study by A.A. Mathews, Inc. for JPL, November, 1977.

9. Gawthorpe, R. (British Railways Board), "Private Communique", June, 1977.

10. Dayman, B. and Kurtz, D., "Experimental Studies Relating to the Aerodynamics of Trains Traveling in Tunnels at Low Speeds", Proceedings of the first International Symposium on the Aerodynamics and Ventilation of Vehicle Tunnels, Organized by BHRA, Canterbury, U.K., April, 1973.

11. "Alleviation of Pressure Pulse Effects for Train Entering Tunnels", a study by JPL for DOT-TSC, 1978.

TABLE 1

TEST VARIABLES

TUBE

Diameter = 5.04 cm
Length = 14, 19½ m

ENTRANCE PORTAL

Perforated

Length = ½, 1, 2 m
Porosity Ratio = 0, 0.125, 0.25, 0.5, 0.75, 1.0

Flared

Length = 1 m
Entrance Area = 2½ times tube area
Porosity Ratio = 0, 0.25

EXIT PORTAL ORIFICE

Diameter = 1, 3, 5 cm

VENT SHAFT

Length = 15 cm
Diameter = 0, 2 (Constant diameter or with orifice), 5 cm

MODEL

Blockage Ratio = 0.25, 0.50, 0.75
Length = 55, 110 cm
Nose = flat and conical
Base = constant diameter and built-up
Body = solid and perforated
Velocity = 12 - 28 m/s

INSTRUMENTATION

Pressure Transients

4 Kistler
3 Statham
1 Kulite

Oscilloscopes

4 Dual-beam

Photo-cell "speed trap"

TABLE 2

TRADE-OFF STUDY
COMPARISON OF APPROACHES
($K PER YEAR)

	TE	BE	PEOPLE		CAPITAL*	Σ **
RESTRICTED SPEED						
Hold To 60 mph Till Past Portal	-3	0	97	(11)∂	0	94
80 - 60 - 80 mph	34	18	45	(5)	0	97
NO SPEED RESTRICTION	0	0	0	(0)	180	18
(200 m Long Perforated Entry Portal						
SEALED CARS (200 CARS)	0	0	0	(0)	20000#	2000

* TOTAL (NOT PER YEAR)

** $\Sigma = TE + BE + PEOPLE + \frac{CAPITAL}{10}$

∂( ) TIME LOST PER ENTRY, SEC

\# GUESTIMATE

TABLE 3

TEST CONDITIONS AND OSCILLOSCOPE SCALES FOR FIGURE 11
(Kulite Pressure Transducer at Station 225; 55 cm long model entering 19½ m long tube)

Run	Entry Length (m)	Portal Porosity (%)	Model Blockage (%)	Approx. Entry Speed (m/s)	Scales Time ms/unit	Scales Pressure kPa/unit
234	Normal		50	24.1	19.3	0.46
235			50	25.4	48.2	0.46
236			25	24.7	19.3	0.18
237			75			1.84
238		50	75			1.84
239			50			0.46
240			25			0.18
241			50		48.2	0.46
242	½				19.3	
243	2					
245	1			20.3		
246	1			14.5		

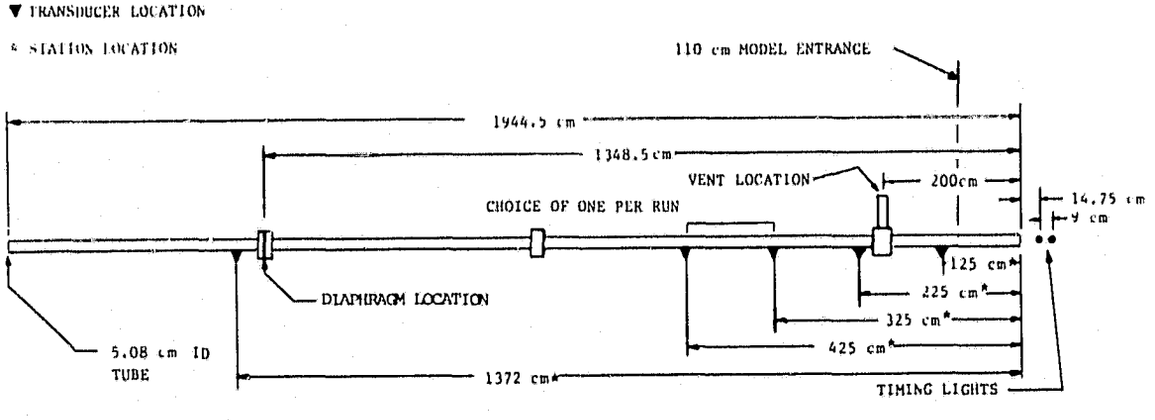

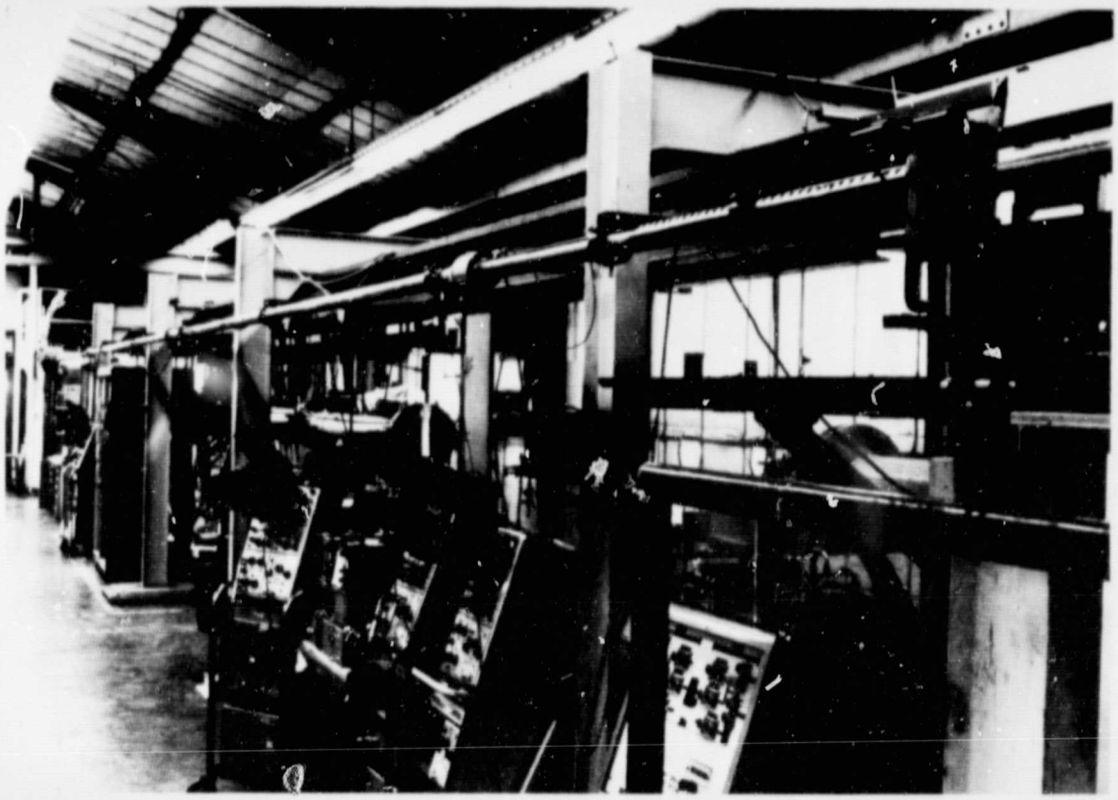

2. Photo of test facility

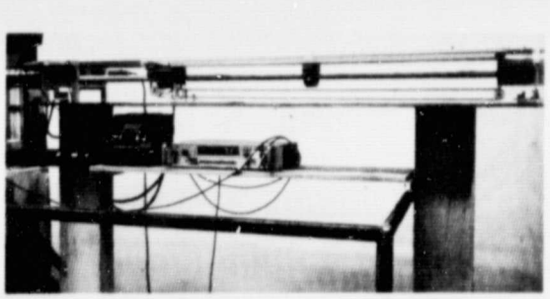

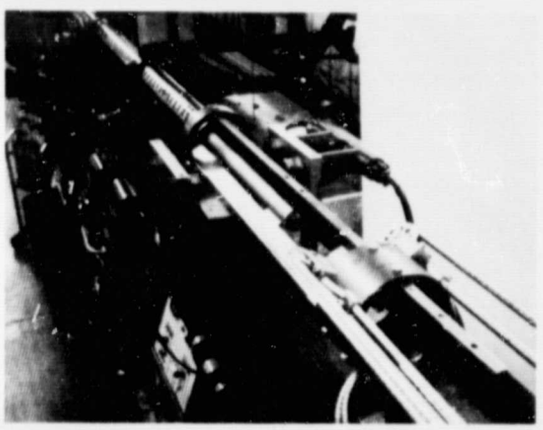

3. Photo of model launcher

a. Side view showing readout for real-time determination of model launch velocity

b. View from above showing model entering tube

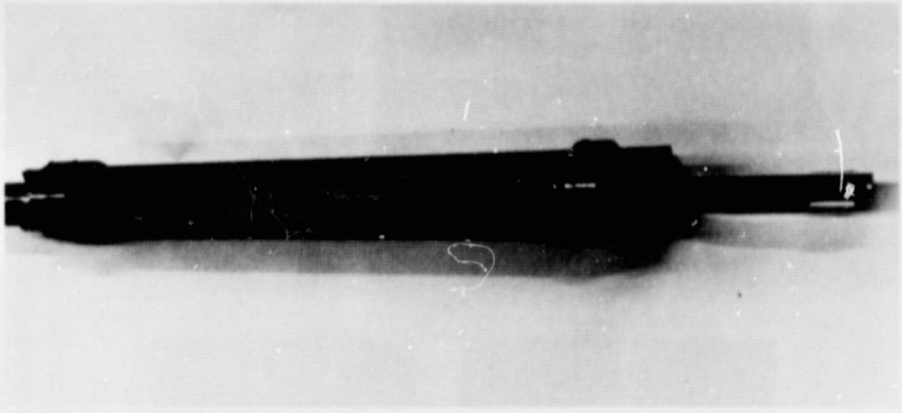

4. Photo of conical entry portal with model having leak holes open

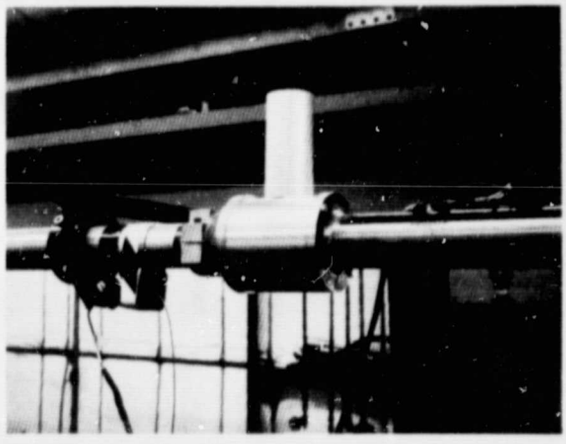

5. Photo of flange containing vent shaft

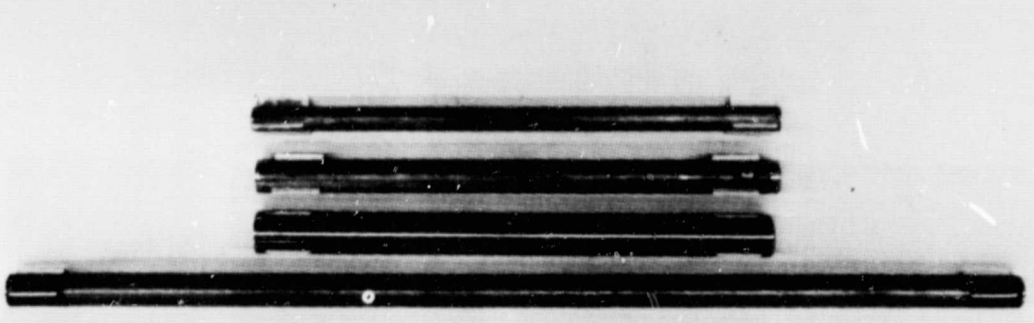

6. Photo of train models
Description of models from top to bottom

Blockage	Length
25%	55 cm
50%	55 cm (leak holes open)
75%	55 cm
50%	110 cm

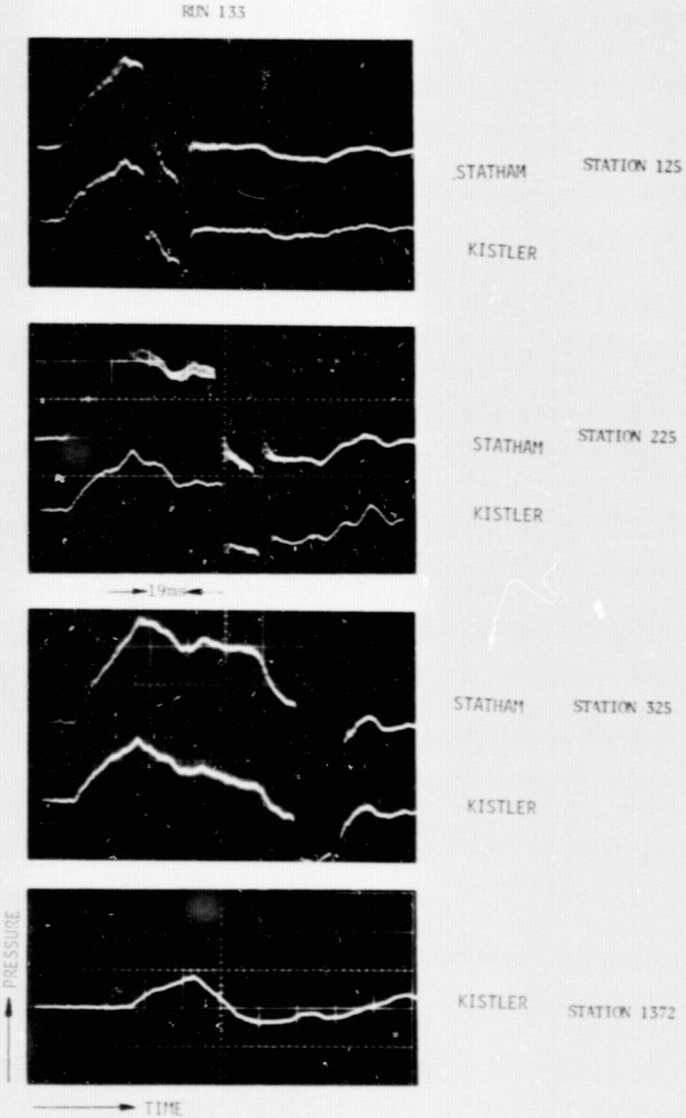

7. Example of normal oscillograph data

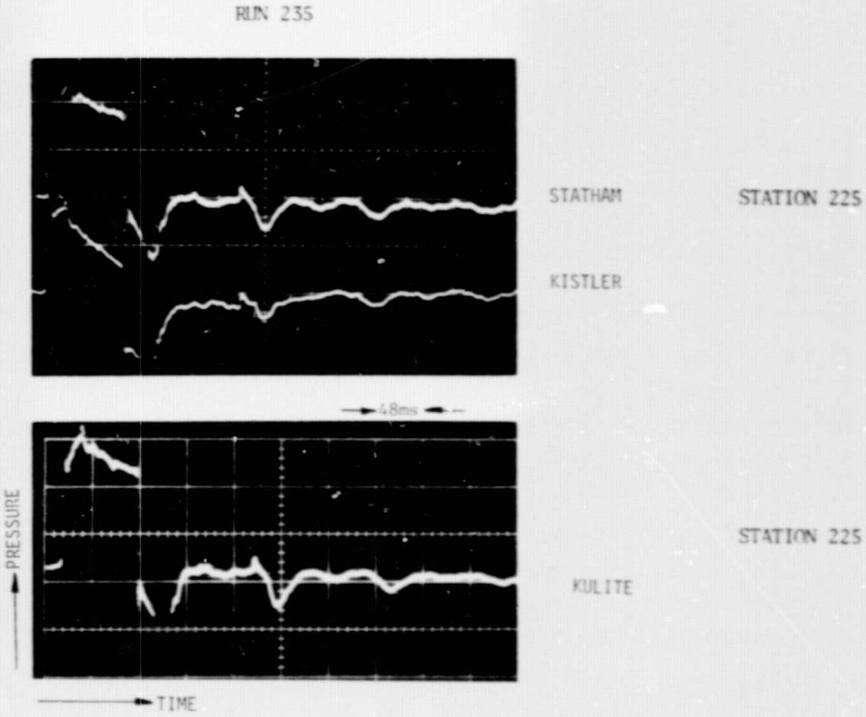

8. Comparison of oscilloscope traces for various transducers

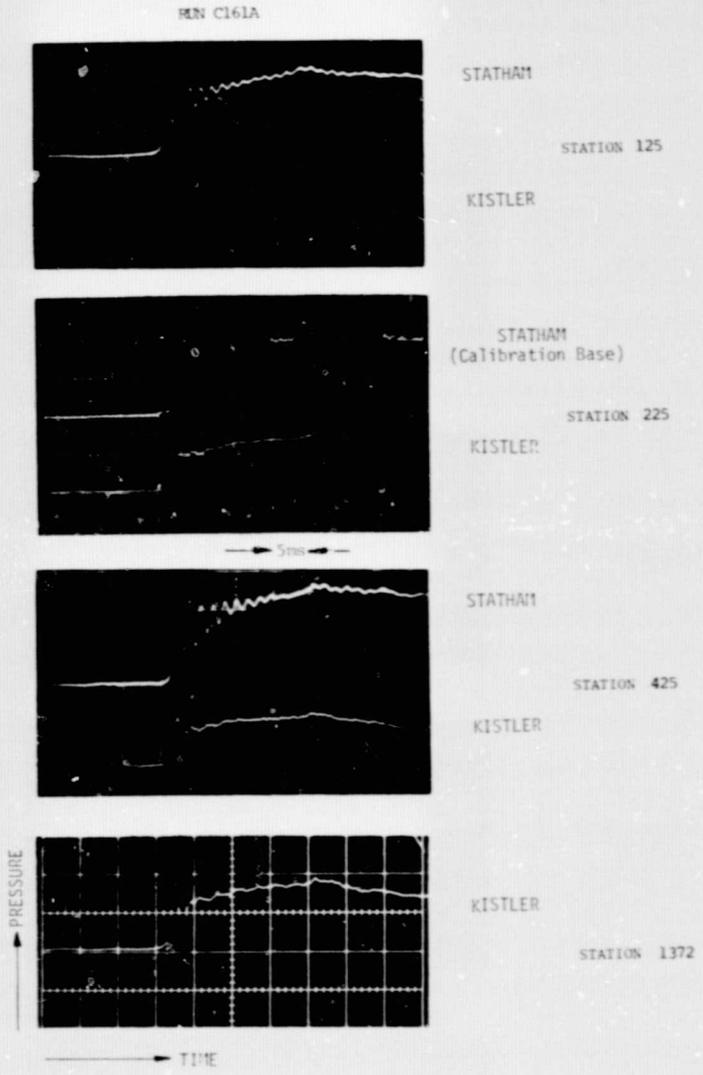

9. Example of trace data used for relative calibrations

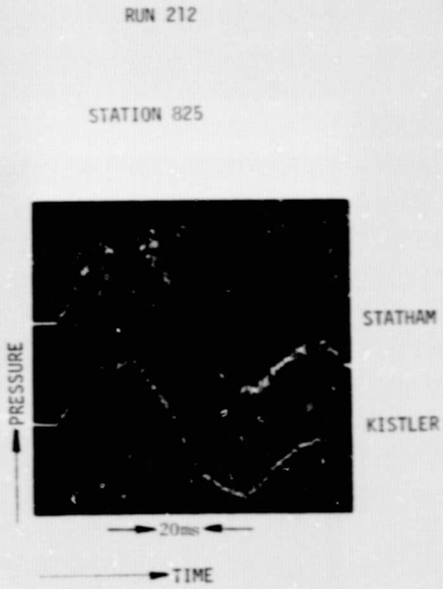

10. Example of diaphragm-burst oscilloscope data

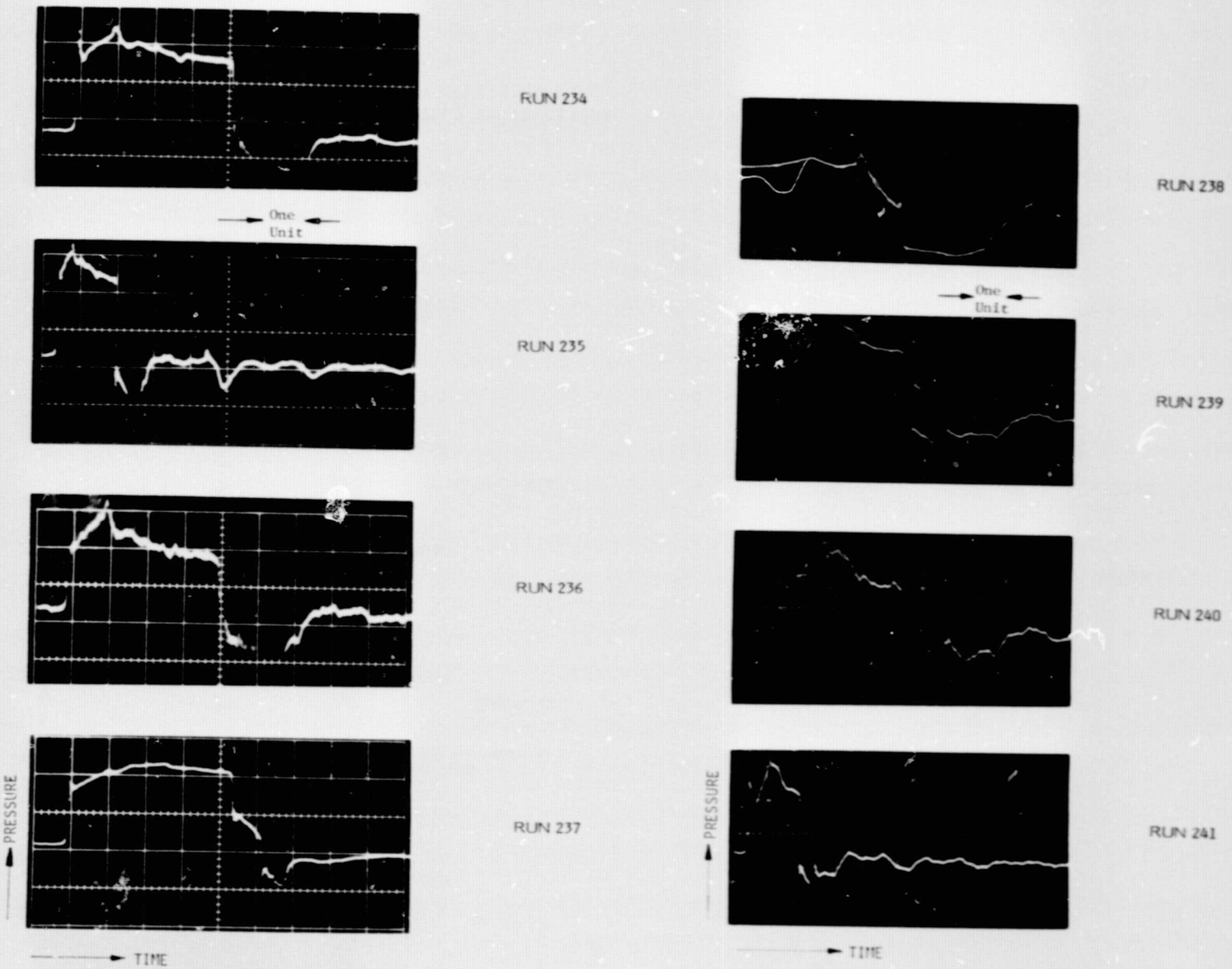

11. Examples of Pressure Traces for Various Test Conditions (Test Conditions are Described in Table 3)

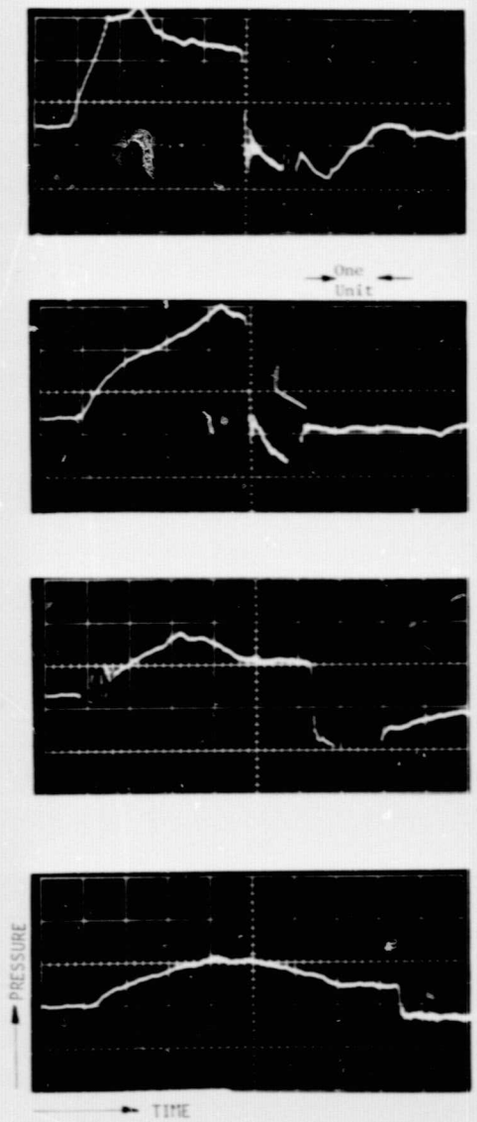

Figure 11. (Continued)

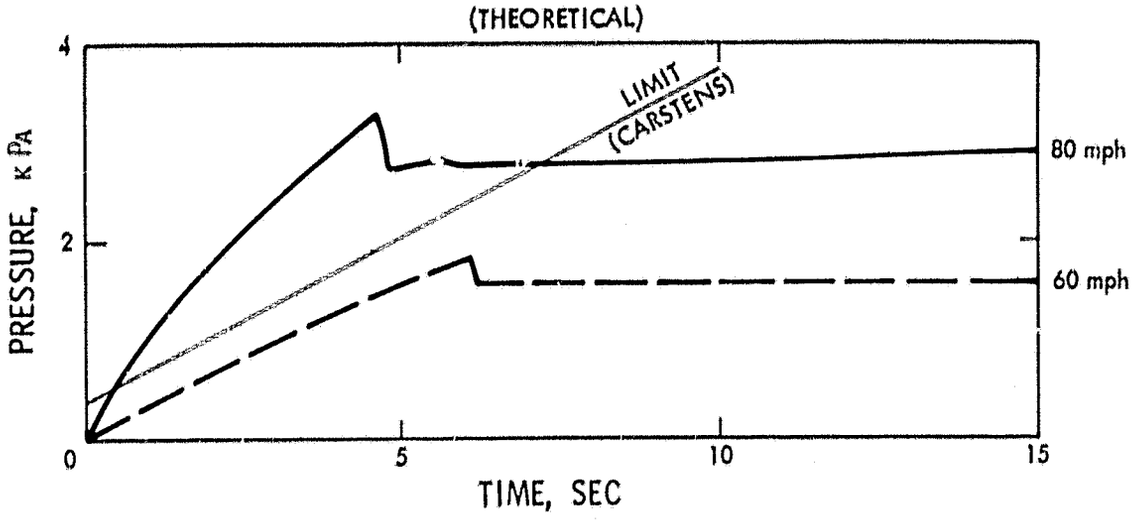

12. Effect of train speed on pressure transients experienced by riders on trains entering normal constant-diameter tunnels (150 m long train of 50% blockage)

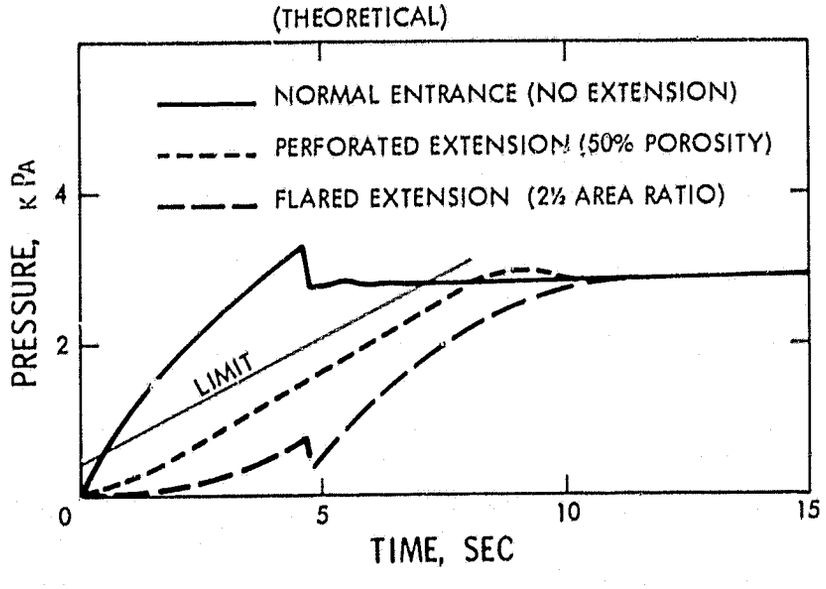

13. Effect of 200 m long portal extension on pressure transients experience by riders on trains entering tunnels (150 m long train of 50% blockage traveling 80 mph)

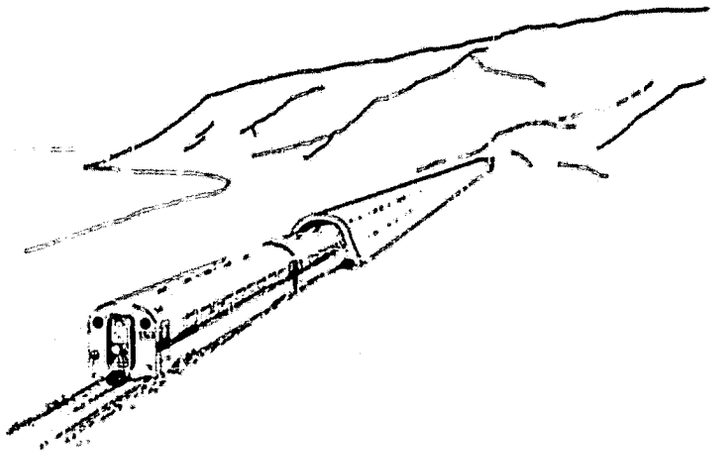

a. Perforated (constant area)

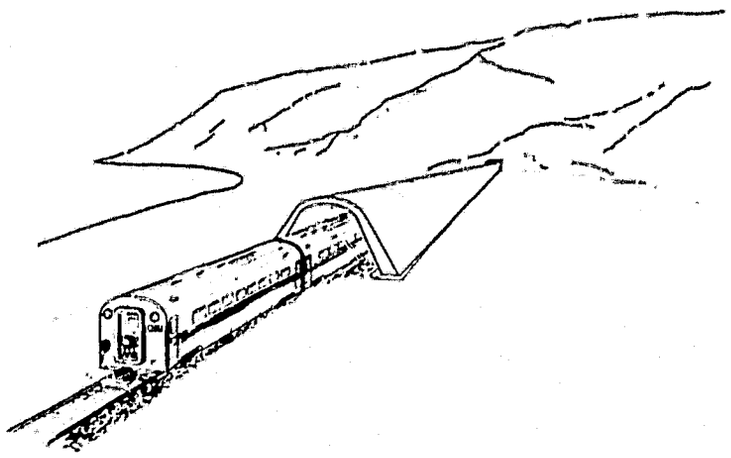

b. Flared (entrance end is $2\frac{1}{2}$ times tunnel area)

14. Drawings of suggested tunnel entry portal extensions

ALLEVIATION OF TUNNEL ENTRY PRESSURE TRANSIENTS: 2. THEORETICAL MODELLING AND EXPERIMENTAL CORRELATION

A.E. Vardy, B.Sc., Ph.D., C.Eng., M.I.C.E.

University of Cambridge, U.K.

B.Dayman, Jr., B.Sc., M.Sc., P.Eng., A.Eng.

Summary

A computer program is used to predict the pressure histories on the walls of a tunnel when a train enters and passes through the tunnel at speed. The program is capable of simulating the velocity and pressure histories in complex tunnel systems during the passage of any number of trains. Comparisons are made with pressure histories recorded by transducers mounted on the wall of the laboratory model described in the first of these two papers. By carefully choosing empirical coefficients in order to give a good fit to the data, excellent correlation is obtained for the basic case of a train in a simple tunnel. The principal features of the pressure histories in a wide range of tunnel configurations are also well simulated using the same empirical data.

Comparisons are also made with full scale measurements obtained in Patchway Tunnel. The correlation is not as good as with the laboratory measurements. However, it is sufficiently close for the accompanying predictions of the influence of various modifications to the tunnel to be regarded as valid. It is shown that there are significant benefits to be gained from entrance modifications, but that these cannot alone provide a complete solution. Account must also be taken of the pressure fluctuations generated during train exit.

NOMENCLATURE

a	cross-sectional area
a_o	area of pores in a unit length of the duct walls
c	sonic velocity
C_D	discharge coefficient
C_F	skin friction coefficient (= shear stress $\div \frac{1}{2}\rho u^2$)
F	skin friction per unit length (+ve in -ve x-direction)
g	gravitational acceleration
k	stagnation pressure loss coefficient
ℓ	length of perimeter of cross section
L	effective wall thickness
$\dot{m}$	mass flux per unit length through duct walls
p	static pressure
t	time co-ordinate
TEPT	Tunnel Entry Pressure Transients (see Ref. 1)
u	air velocity (axial)
u^*	air velocity in annulus relative to train
$\bar{u}$	axial component of velocity of flow through wall
U	train speed
v	lateral component of velocity of flow through wall (inflow = +ve)
x	distance co-ordinate
z	elevation
β	train/tunnel blockage ratio
γ	ratio of specific heats of air
ρ	mass density of air

Suffices

AT	atmospheric conditions
N	train nose
T	train tail
t	tunnel
v	train (vehicle)

1 INTRODUCTION

One of the main purposes of the TEPT project (Ref. 1) is to provide experimental data with which to test the validity of theoretical models of train/tunnel aerodynamics. In this paper, comparisons are made between some of the data and a computer program based on the pseudo-isentropic approach proposed originally by Fox and Henson (Ref. 2).

The computer program is capable of simulating all of the situations covered in the experimental programme except those dealing with porous trains. In addition, it can take account of any number of trains in the tunnel simultaneously, and these may pass alongside one another. Separate investigations will be needed before the validity of the additional facilities is proven. However, it may be inferred from the good agreement between theory and practice that is exhibited in this paper that the basic approach is sound. In particular, the additional accuracy that might be achieved by using a program based on non-isentropic relationships is not likely to be sufficient to justify the extra complexity involved.

The capabilities and the theoretical basis of the program are outlined in section 2, and its predictions are compared with experimental measurements in sections 3 - 6. Attention is drawn to several discrepancies and these are found to be in part due to theoretical inadequacies and in part due to experimental errors that inevitably creep into an extensive laboratory programme. Section 7 contains information on the implications of the work at full scale. Examples are presented in which the influence of tunnel modifications on the pressure histories experienced by passengers can be seen.

2 THE COMPUTER PROGRAM

The computer program is new. It is similar in principle to that used by Vardy (Ref. 3), but it is more efficient and it has greater capabilities. The flexibility offered by the program can be summarised as follows:

A. Tunnel system

1. There may be any number of tunnels joined together to form any desired network.
2. Any number of ducts may meet at a single junction. Hence airshafts, cross-passages and cross-overs are easily accommodated. At such junctions, stagnation pressure loss coefficients may be input for every possible flow combination.
3. Interventing between adjacent tunnels may be specified in the form of discrete adits of any length and cross-section. At present, perforated dividing walls may not be specified, but this facility could be made available.
4. The tunnels may have stepped or gradual area changes.
5. The tunnels may have perforated walls connecting to the atmosphere. In this case, account is taken of the dimensions of the ventilating holes.
6. Changes in elevation may be specified along tunnels and airshafts.
7. Local flow restrictions may be specified at any position. To simulate sliding doors, etc., temporal variations of the amounts of the restrictions can be specified.
8. Ventilation fans and other boundaries with predetermined pressure-discharge relationships may be stipulated at any position in the tunnel system.

B. Trains

1. The trains are regarded as constant area, impervious objects. Local increases in area may be specified at the nose and tail in order to correctly reproduce the pressure differences at these locations. In particular, this permits the simulation of built-up tails.
2. The speed history is specified in any one of three forms: a) constant speed, b) predetermined acceleration history - permits stopping, starting, reversing, etc. or c) acceleration is determined from aerodynamic drag.
3. There may be any number of trains. Each may be routed through the tunnel system in any desired manner. Two (but not more) trains are permitted alongside one-another in any tunnel.
4. Stationery trains may be present anywhere inside the system before a run begins. They may subsequently be routed through the system in any desired manner.

2.1 Theoretical basis

The airflows are regarded as one-dimensional, unsteady and compressible, and account is taken of skin friction on the tunnel and train surfaces. Consider the control volume depicted in Figure 1. By assuming that the pressure and density fluctuations throughout the system satisfy isentropic relationships, the continuity and momentum equations can be combined into the characteristic forms

$$\frac{2}{\gamma-1}\frac{dc}{dt} \pm \frac{du}{dt} = -\frac{cu}{a}\frac{da}{dx} \mp \frac{F}{\rho a} + \frac{c\dot{m}}{\rho a} \mp (u-\bar{u})\frac{\dot{m}}{\rho a} \mp g\frac{dz}{dx} \qquad (1)$$

which are valid only in the directions

$$\frac{dx}{dt} = u \pm c \qquad (2)$$

respectively. When the tunnel walls are perforated, the lateral mass influx per unit length $\dot{m}$ is deduced from the unsteady form of the isentropic Bernoulli equation,

$$\frac{1}{\gamma-1}(c^2 - c_{AT}^2) + \tfrac{1}{2} v|v| = g(z-z_{AT}) - L\frac{\partial v}{\partial t} \qquad (3)$$

in which the lateral velocity v is related to $\dot{m}$ by

$$\dot{m} = C_D \rho a_o v \qquad (4)$$

and a_o is the area of the holes in the walls of a unit length of the duct. L is the effective wall thickness.

The skin friction on the tunnel walls is assumed to satisfy

$$F_t = \tfrac{1}{2} C_F \rho \ell_t u|u| \qquad (5)$$

in which C_F is the friction coefficient and ℓ_t denotes the perimeter of the tunnel cross-section. A similar expression is used to describe the skin friction on the train surface, but the appropriate velocity is then measured relative to the train. The determination of suitable values for the coefficient is described in section 3.

Equations (1) through (5) are applicable at all times throughout the tunnel system. They are subject to local boundary conditions at the tunnel portals, at junctions, at restrictions and at the nose and tail of each train. At these positions, the above equations are supplemented by steady-state continuity and Bernoulli expressions describing the instantaneous local flows relative to the boundary.

In addition to these conventional boundary conditions, a facility is included in the program in order to permit complete ducts to be regarded as boundaries. In this case, the unsteady form of the Bernoulli equation is used to describe the flow through the duct. This feature permits the option of including airshafts and cross-passages without regarding them as ducts in which the characteristic equations must be applied. A similar method of analysis is commonly used to simulate the influence of surge tanks in hydraulic pipe networks. All the results presented for airshafts in this paper are obtained in this manner. Comparisons have been made with solutions using the characteristic analysis along the shafts, and negligible differences exist because the shafts are so short.

2.2 Numerical considerations

The solution of one-dimensional unsteady flows by the method of characteristics is well documented, and there is no need to discuss this in detail. Attention is drawn, however, to certain features of the numerical solution that are not yet in widespread use.

The fixed-grid method of solution is used. However, different grid sizes may be

specified in different tunnels. In particular, this permits the use of closely spaced grid points in regions of special interest - e.g. flares and perforated tubes - in conjunction with wider spaced grid points in simple tunnels. The same time interval of integration is used throughout the network. It satisfies

$$\Delta t = \frac{\Delta x}{c} \qquad (6)$$

in which Δx is the largest grid size in the system. This apparently implies that Δt will greatly exceed the usual stability limit, but such is not the case if care is taken in the manner of interpolating data. More information can be found in Refs. 4 and 5. In the latter, Wiggert and Sundquist give a useful error analysis. However, the scheme has been further developed since these papers were written, and more information will be published in the near future.

3 BASIC DATA

The most common event in full-scale systems is that of a simple train travelling through a simple tunnel. It is imperative that any analytical tool which is to be used by designers should be capable of simulating this basic case with good accuracy.

Several runs are shown in Fig. 2 in which the continuous lines represent theoretical predictions and the broken lines are experimental traces. In each case the comparison is made with pressures at a recording station which is 2·25 m downstream of the entrance portal. The run number corresponds with the value given in Ref. 1 and the velocity U_o is the assumed speed of the vehicle at nose-entry. The program automatically allows for the deceleration of the train due to aerodynamic drag, but no allowance is made for the resistance of the vehicle skids on the tunnel wall.

The empirical data used in the computer program in order to produce the theoretical curves is listed in Table 1. There is assumed to be no loss of stagnation pressure as the air flows past the nose into the annulus around the train, but a stagnation pressure loss which satisfies

$$\Delta p_T = k_T \tfrac{1}{2} \rho (u^*)^2 \qquad (7)$$

occurs as the flow expands from the annulus into the open tunnel at the tail of the vehicle.

The agreement between theory and experiment is generally very good, but this is of course partly due to the choice of empirical data which gives the 'best-fit' to the experimental results. However, there are various features of special interest to which attention should be drawn. Firstly, the stagnation pressure loss coefficient at the tail of the train appears to satisfy

$$k_T \simeq \beta^2 + 0{\cdot}1 \qquad (8)$$

in which β denotes the train blockage ratio. No explanation is offered for this result, but it is useful to observe that the expression $k_T = \beta^2$ can be deduced by assuming that the pressure on the trailing face of the train is equal to the pressure at the rear of the annulus (Ref. 1). The excess of the measured k_T over β^2 is a consequence of the reduced pressure on the trailing face of the vehicle (Ref. 6).

The use of skin friction expressions such as (5) merits discussion. It is highly unlikely that the coefficient C_F can be truly constant in an unsteady flow situation. Also, the appropriate value for the tunnel coefficient in the annulus alongside the train is expected to be different from the value in the unblocked tunnel. However, there is no way of deducing the actual values from the presented data. In order to illustrate this difficulty, Fig. 1 includes a run labelled 100* in which the tunnel and train friction coefficients are 0·0225 and 0 respectively. The total skin friction in the annulus is approximately the same as for run 100, but this is wholly on the

tunnel surface. By inspection, it is seen that the 'agreement' between theory and experiment is approximately the same for both runs.

Runs 184 and 191 deal with a train which has an identical cross-section, but which is twice as long (1·10 m). The tabulated skin friction coefficients are used for these runs and, in particular, run 191 has been used to select the best value of the tunnel skin friction. For simplicity, the same value is used for the tunnel walls in the annulus even though it is recognised that this may be an unrealistic representation of the real phenomenon. As explained above, the consequences of this approximation are not serious because the overall result is not sensitive to the distribution of skin friction in the annulus.

A final comment about the friction coefficients is appropriate. The insensitivity of the results might disappear when experiments involving a wider range of speeds are considered. In this case, it is expected that there will be a need to either (a) vary the train coefficient with speed or (b) use a constant value for the train coefficient, but in conjunction with a tunnel coefficient that is different from the value used in the open tunnel.

4 EXTENDED ENTRANCE REGIONS

Two extended entrance regions have been simulated. Fig. 3 includes run 178 in which a 0·55 m long train entered the tunnel through a 1m long conical flare. The agreement between theory and experiment is reasonable, but attention is drawn to the choices of empirical input. The stagnation pressure loss coefficient at the tail of the vehicle has been assumed to satisfy the expression (8) which was itself deduced from runs with parallel sided tunnel walls. Also, the tunnel skin friction coefficient in the flare has been chosen as 0·025. The need for this modification is not fully understood, but two possible reasons are put forward. Firstly, the friction coefficient in the annulus is greater for low blockage ratio trains than for high ones - see Table 1. Since the train coefficient is retained as 0·005 throughout run 178, a higher tunnel coefficient might be expected. Secondly, the computer program takes no account of distributed pressure losses other than those due to friction. In practice, there will be an additional loss if the flare fails to act as an efficient diffuser for the air in the annulus where the flow is backwards relative to the tunnel as well as relative to the train.

The influence of a 0·95 m long perforated entrance region is also simulated satisfactorily (run 186). The perforations are actually four 1/8th inch (3·175 mm) diameter holes spaced around the circumference at each of 32 sections at 3cm spacings along the tube, but in the computer simulation the holes are regarded as being evenly distributed along the whole 0·95 m. The total area of the holes is 50% of the cross sectional area of the tunnel, but the effective area of the vena contractas is smaller. In order to take account of this difference, a discharge coefficient $C_D = 0{\cdot}61$ is used in equation (4).

One feature that is clearly illustrated by this run is that the tail-entry wavefront is not elongated in the same way as the nose-entry wavefront. This is not a matter of great concern as far as personnel inside the tunnel are concerned, but it is important for passengers, especially those near the rear of the train. They will experience a tail-entry wavefront which is only slightly smaller than that expected in an unmodified tunnel.

For the sake of completeness, run 181 is also simulated. In this case, the flare used for run 178 is also perforated by half as many holes as were used for run 186. The features exhibited in this run are an understandable combination of those discussed for the flared and perforated regions alone.

5 AIRSHAFTS

In run 160, the 50·8 mm ID tunnel is equipped with a 0·15 m long, 20 mm ID airshaft, 2m from the entrance portal. The shaft complicates the pressure histories by providing an

extra discontinuity at which the various wavefronts can reflect and at which additional wavefronts are generated when the train passes. It is the resulting superposition of the many wavefronts that is recorded at the pressure transducer, and there is therefore considerable scope for apparently large discrepancies due to small errors in the predicted arrival times of different wavefronts. Given this difficulty, considerable confidence can be placed in the ability of the program to simulate the influence of the shaft.

Similar conclusions may be drawn for run 156 which is similar to run 160 in all respects except that the shaft is 50 mm ID. Of course, a much greater mass flux passes through the larger bore shaft and so the mean pressure level in the tunnel is much smaller. Nevertheless, the overall influence of the shaft is essentially expressible in terms of pressure wave activity.

In run 156 (and also to a lesser extent in run 160), the predicted pressure fluctuations upstream of the shaft (not shown) are greater than the measured values. There are two possible explanations for this effect. The most probable cause is that the dispersion of the wavefronts is underestimated during the early stages of their transmission and during reflections at the several boundaries. However, it is also possible that there was an experimental error of unknown origin. The latter possibility is mentioned because the previous run (155) certainly contains an unexplained experimental error. This run is shown in Fig. 3, and the error can be deduced by comparison with run 100 in Fig. 2. Except for the different scales, these runs should be almost identical for the first 0·10 seconds. In particular, the measured nose-entry and tail-entry wavefronts are smaller than expected in run 155, features that are also exhibited in run 156.

5.1 Partially blocked airshafts

Runs 162 and 163 are shown in Fig. 4. In both of these, the 50 mm bore shaft is used, but it is partially blocked at the bottom and top respectively. This configuration was shown by Vardy and Fox (Ref. 7) to have advantages in comparison with constant-bore shafts when these are unusually long. The experimental set-up dealt with very short shafts and so this effect is not apparent. Nevertheless, it is useful to demonstrate that the computer program can simulate this situation as well as the simple shaft.

5.2 Airshaft and perforated entrance region

In runs 166 and 167, the 50 mm and 20 mm bore shafts are used in conjunction with the perforated entrance region. Not surprisingly, the agreement is generally as good for this combined arrangement as for the tunnel modifications alone. However, the magnitude of the wavefront generated when the nose passes the shaft (0·075 s) is underestimated. No complete explanation has been found for this result, but it is presumed that the mass flux through the shaft is wrongly estimated during the period when the train passes the base of the shaft. The geometrical configuration at this time is somewhat complex and it is by no means certain that a similar result would obtain at full scale.

6 LOCAL RESTRICTIONS

In addition to simulating conventional tunnel configurations and extended entrance regions, the computer program can model local flow restrictions. These may be present at any location within the tunnel network, and they may be adjusted during the train journey if required. The use of such restrictions at a tunnel exit portal has been shown by Vardy (Ref. 8) to be potentially very useful.

Run 189 illustrates the influence of an exit portal restriction at the end of the 18·445 m long tunnel when a 1·10 m train passes through. In the experimental rig, the restriction was formed by cutting a 10 mm hole in a sheet of cardboard and by taping the card to the tunnel portal. Because the train was larger than the orifice, care was taken to use relatively little adhesive tape so that the vehicle could safely remove the blockage during exit.

The influence of this restriction can be seen by comparing run 189 with run 184 (Fig. 2) in which there was no exit restriction. The reflections of the wavefronts generated during train entry begin to arrive at the transducer from the exit portal almost exactly 0·10 secs after nose-entry. Since the restriction is slightly greater than the optimum value, the reflected nose-entry wavefront causes compression in run 189 even though it causes decompression in the basic case (run 184).

The restriction is simulated as a simple orifice through which the local instantaneous flow is assumed to satisfy steady-state formulae. However, the agreement between theory and experiment is achieved by assuming that the vena-contracta downstream of the orifice is 10 mm in diameter. This has been found to be necessary by simple trial and error even though the true orifice diameter is 10 mm. The obvious inconsistency is attributed to leakage between the card and the tube, but the error was not discovered until after the completion of the experimental programme.

It can also be argued that considerable benefit may be expected if the stagnation pressure loss at the tail of the vehicle is increased (Ref. 8). A simple way of achieving this objective in a laboratory circumstance is by locally increasing the vehicle cross-section at the tail. Several runs were carried out with this arrangement and one such example is illustrated in run 207. The final 47·6 mm of the 550 mm train was a truncated cone in which the diameter increased linearly from the standard value of 34·9 mm to 44·5 mm. This increase is considerably greater than the optimum value and it leads to a strong compression wavefront at tail-entry (approx. 0·025 secs).

In order to simulate this configuration, the average pressure on the rear face of the vehicle is assumed to be equal to that at the position of maximum blockage. This leads to a satisfactory agreement between theory and experiment, but some overestimation of the pressure is apparent before the train passes. The cause of this error has not been established, and it is not also present at the upstream transducer (not shown). However, this is a matter of little concern because the overestimation is small and the blockage is far greater than the optimum value. Additionally, this particular method of inducing the stagnation pressure loss might not be appropriate at full-scale.

7 FULL-SCALE IMPLICATIONS

The results obtained from the experimental model do not apply directly to all full-scale situations because the empirical coefficients differ from one location to another. Comparisons are therefore also presented between computed predictions and measurements in Patchway Tunnel reported by Gawthorpe & Pope (Ref. 9). This data is especially valuable because no complications arise due to airshafts or passing trains, etc.

The agreement presented in Figure 5 is disappointing. The first 8 seconds (approx.) are well simulated, but the subsequent pressure fluctuations are overestimated. Similar difficulties were reported by Gawthorpe & Pope and also by Hawarth (Ref. 10) who included non-isentropic effects. By inspection, it is seen that the nose-entry wavefront and its reflection from the exit portal are well modelled, but that the subsequent reflection from the entrance portal is overestimated. It is concluded that there is far more dispersion in the annulus than the theoretical models predict, and this is believed to be due to the influence of unsteadiness on the friction coefficients. Nevertheless, the agreement is sufficiently good for the overall influence of various tunnel modifications to be investigated. Values of 0·0075 and 0·0175 are used for the skin friction coefficients on the tunnel and train surfaces respectively. Additionally, the stagnation pressure loss at the tail is assumed to satisfy equation (8) and the nose coefficient is 0·40. These values are all different from those used by Gawthorpe & Pope.

Figures 6(a, b & c) depict the pressure histories which would be experienced by passengers near the front and rear of a train on a typical journey. The histories are compared with those which would be experienced if the tunnel was equipped with (a) a 200 m flared entrance region upstream of the original portal, (b) a 200 m perforated entrance region with a total hole area equal to 75% of the tunnel cross-section, and (c) the same perforated region and also a 50 m long, 2m diameter airshaft, 200 m downstream of the original portal. In order to simulate a realistic case, the train is assumed to be 200 m long. All other parameters are the same as those used in Fig. 5.

By inspection, the influences of the flared and perforated extensions are very similar. The peak pressure generated during train entry is reduced by about 25% and the subsequent pressure fluctuations are considerably damped. However, there is very little effect on the pressure histories during train exit. Indeed, the small influence that is apparent is detrimental rather than helpful. The inclusion of an airshaft in addition to the perforated extension leads to a total reduction of about 45% in the peak pressure during train entry, but again has little influence on the train exit disturbances. Indeed, passengers at the tail of the vehicle now experience a greater pressure change during exit than do passengers at the front during entry. It may be concluded that there is little point in further improving the tunnel entrance configuration unless attention is also paid to reducing either the magnitudes or the rates of change of the pressure fluctuations generated during train-exit. Nevertheless, the potential improvement of about 45% in the entry effect is a valuable benefit.

8 CONCLUSIONS

A computer program has been described which is capable of simulating the unsteady pressure and velocity histories throughout a tunnel network during the passage of trains. The network may be complex and the tunnels may be flared and/or perforated in addition to having step-area variations and airshafts, etc. The trains may pass along any route with any speed history.

Good agreement has been demonstrated between the computed predictions and experimental measurement of the pressures in the laboratory apparatus when trains pass through a simple tunnel. Satisfactory agreement has also been obtained for the trains passing through tunnels equipped with flared and perforated extension tubes and with airshafts. In particular, the principal features that distinguish these pressure histories from those in a simple tunnel are well simulated. Confidence is placed in the ability of the program to predict pressure histories in tunnels other than the laboratory model.

Less good agreement has been demonstrated with measurement obtained in Patchway Tunnel. However, the agreement is sufficiently close for the predictions of the influence of tunnel modifications to be regarded as reliable. Flared or perforated entrance regions are shown to yield reductions of the order of 25% in the peak pressure experienced by passengers during train-entry. The additional inclusion of an airshaft in the upstream section of the tunnel is shown to increase the improvement to about 45%. Further improvements would not be cost-effective because the pressure fluctuations associated with train entry are already less than those due to train exit.

REFERENCES

1. JPL staff: 'Tunnel Entry Pressure Transients'. U.S. Dept. Transp. Rep. No. DOT-TSC-UMTA-78-xx-1,2. (1978).

2. Fox, J.A. and Henson, D.A: 'The prediction of the magnitudes of pressure transients generated by a train entering a single tunnel'. Proc. Inst. Civ. Engrs., 49, pp. 53-69. (May 1971).

3. Vardy, A.E: 'The use of airshafts for the alleviation of pressure transients in railway tunnels'. Proc. 2nd int. Symp. on the Aerodynamics and Ventilation of Vehicle Tunnels. Organised by BHRA. Cambridge, U.K. (March 1976).

4. Vardy, A.E: 'On the use of the method of characteristics for the solution of

unsteady flows in networks'. Proc. 2nd int. Conf. on Pressure Surges. Organised by BHRA. London, U.K. (Sept. 1976).

5. Wiggert, D.C. and Sundquist, M.J: 'Fixed-grid characteristics for pipeline transients'. J. Hyd. Div. ASCE, 103, pp. 1403-1416.

6. Dayman, B. Jr. and Kurtz, D.W: 'Experimental studies relating to the aerodynamics of trains travelling in tunnels at low speeds'. Proc. 1st int. Symp. on the Aerodynamics and Ventilation of Vehicle Tunnels. Organised by BHRA. Canterbury, U.K. (April 1973).

7. Vardy, A.E. and Fox, J.A: 'A new airshaft design for railroad tunnels'. ASHRAE J., pp. 41-46. (Feb. 1978).

8. Vardy, A.E: 'Flow restrictions in railway tunnels'. Cambridge University Engrg. Dept. Rep. No. CUED/A.Aero/TR6. (1978).

9. Gawthorpe, R.G. and Pope, C.W: 'The measurement and interpretation of transient pressure generated by trains in tunnels'. Proc. 2nd int. Symp. on the Aerodynamics and Ventilation of Vehicle Tunnels. Orgnanised by BHRA. Cambridge, U.K. (March 1976).

10. Harworth, F: 'Unsteady flows in tunnels' (Theorie instationarer Vorgange im Tunnel). Proc. Int. Seminar on the Aerodynamics of High Speed Railways. Organised by DFVLR Institute for Fluid Dynamics. Gottingen, Germany. (June 1978).

TABLE 1 Empirical coefficients

β	C_F (tunnel)	C_F (train)	k_N	k_T	β^2
0.250	0.010	0.010	0	0.163	0.0625
0.472	0.010	0.005	0	0.325	0.223
0.764	0.010	0.001	0	0.685	0.584

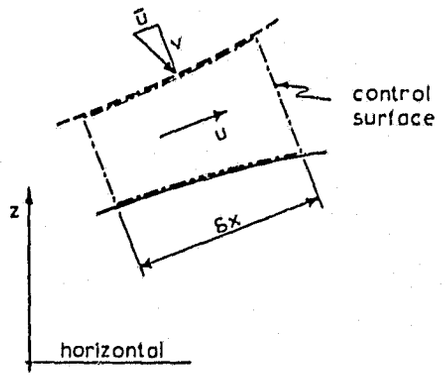

Fig. 1 Definition sketch for flow through an elemental control volume

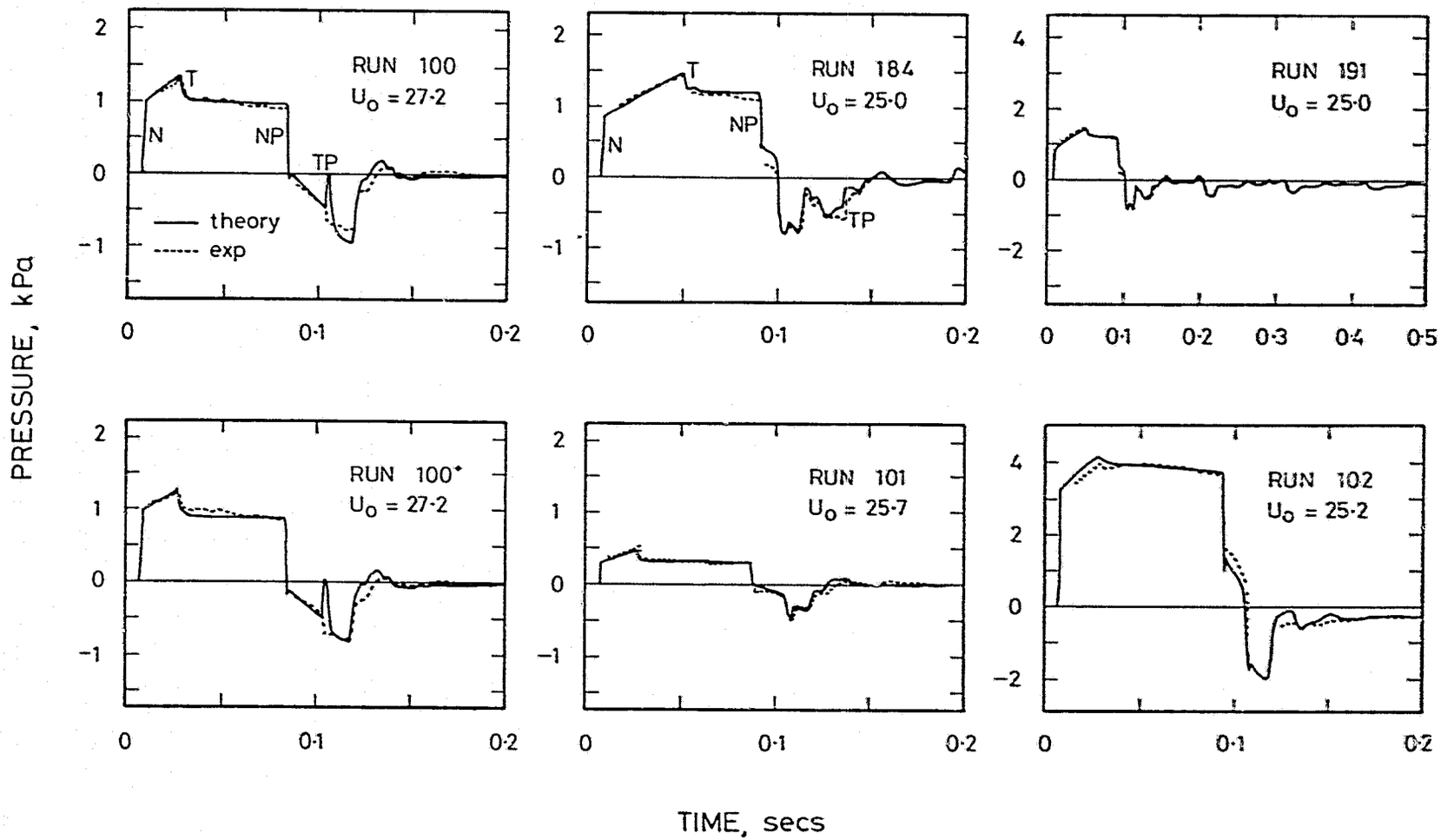

Fig. 2 Comparison of theoretical (————) and experimental (----------) pressure histories 2.25m from the tube entrance: basic cases.

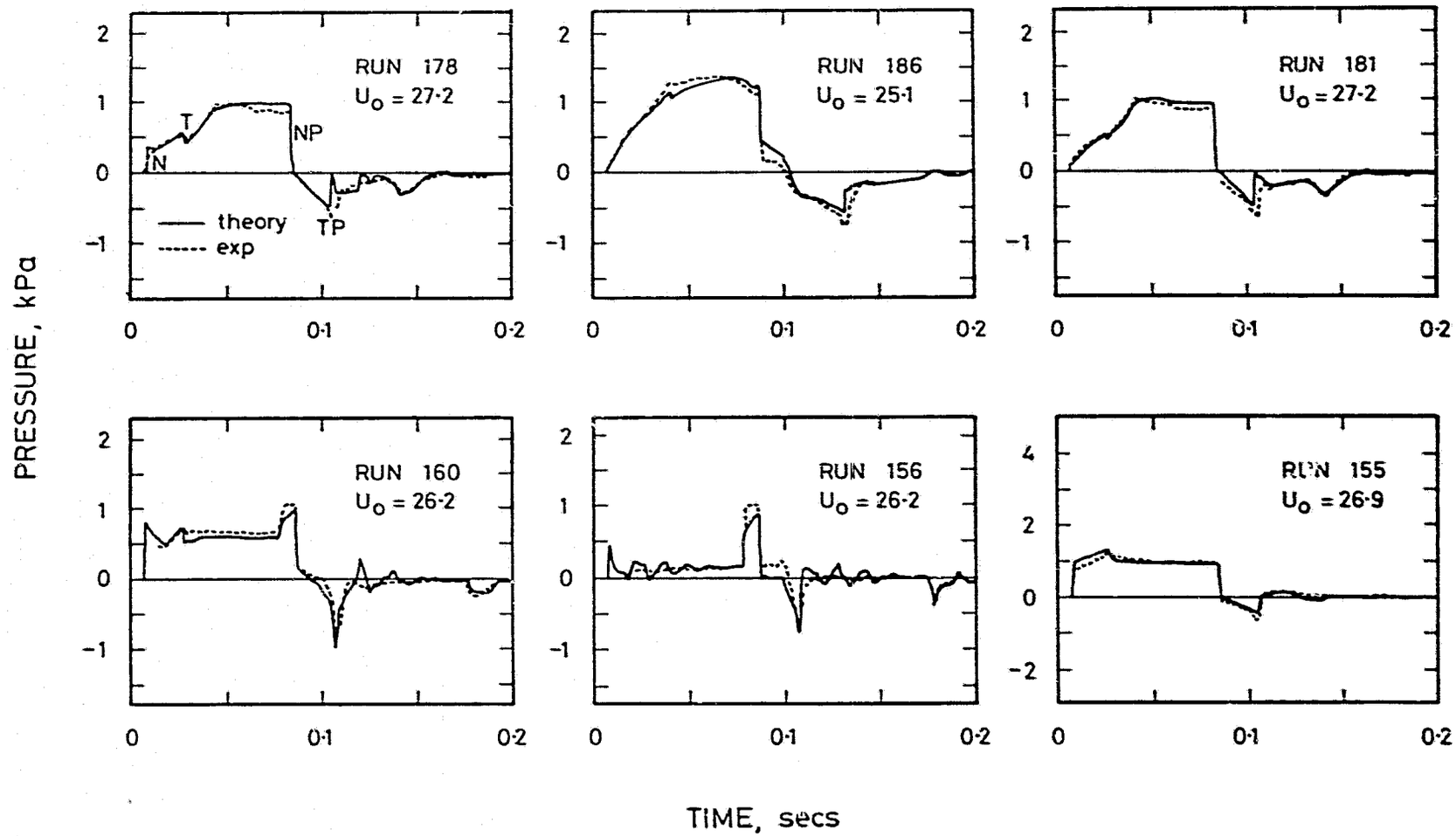

Fig. 3 Comparison of theoretical (————) and experimental (----------) pressure histories 2.25m from the tube entrance: extended entrance regions and airshafts.

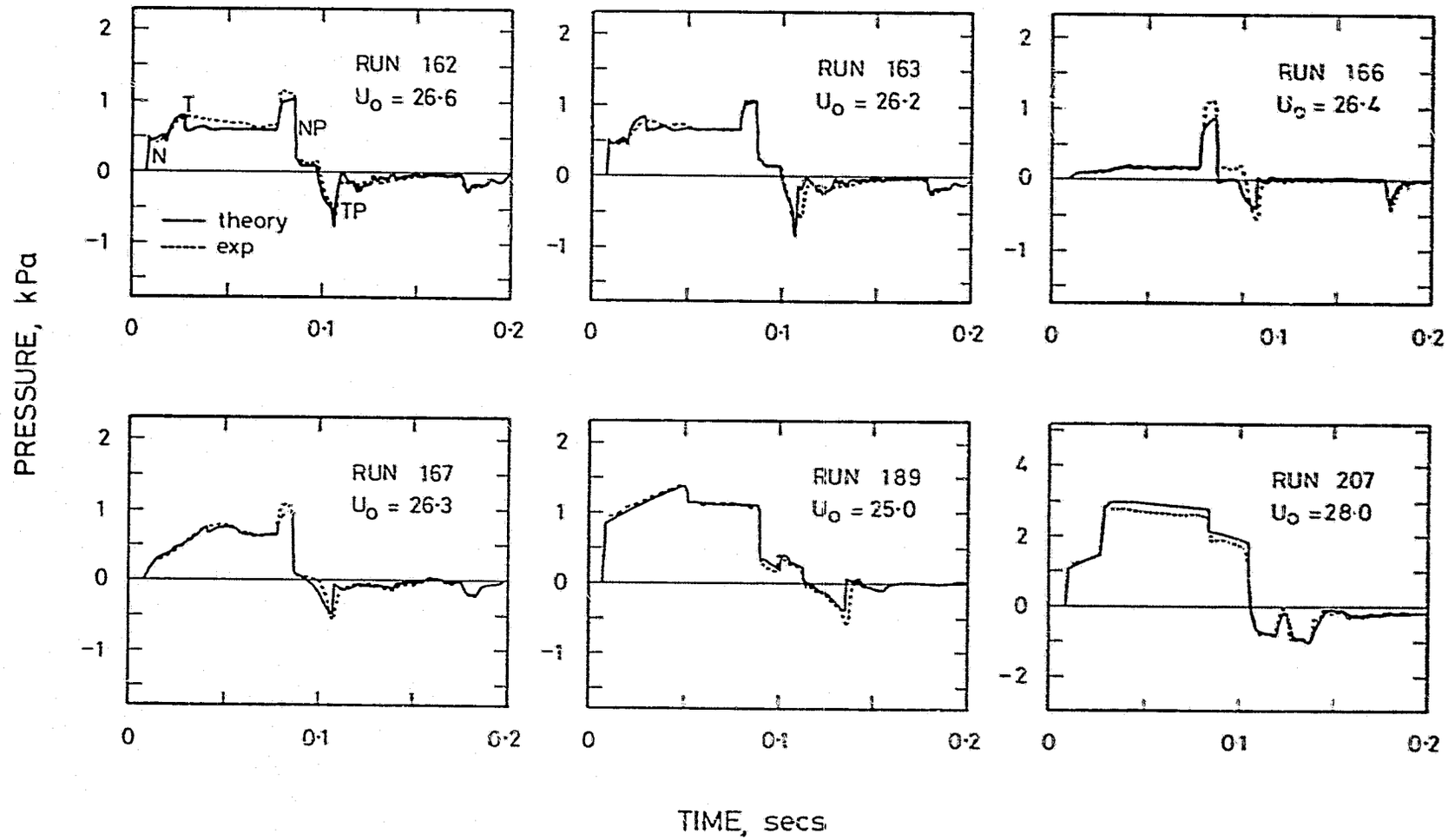

Fig. 4 Comparison of theoretical (————) and experimental (----------) pressure histories 2.25m from the tube entrance: composite tunnel modifications and local restrictions.

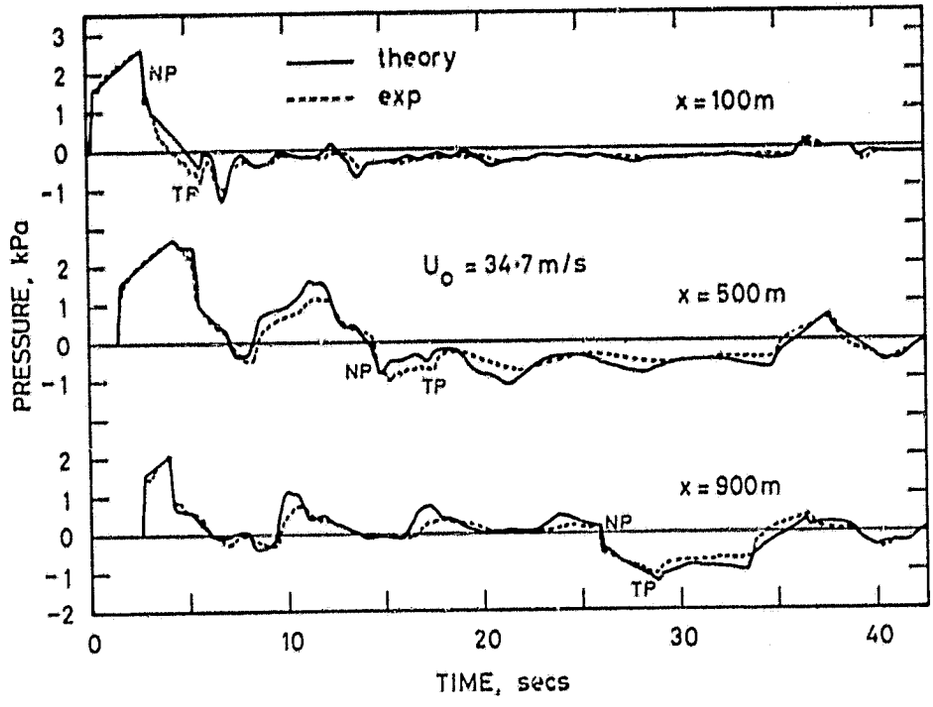

Fig. 5 Comparison of theoretical (————) and experimental (----------) pressure histories in Patchway Tunnel (after Gawthorpe & Pope, Ref. 9).

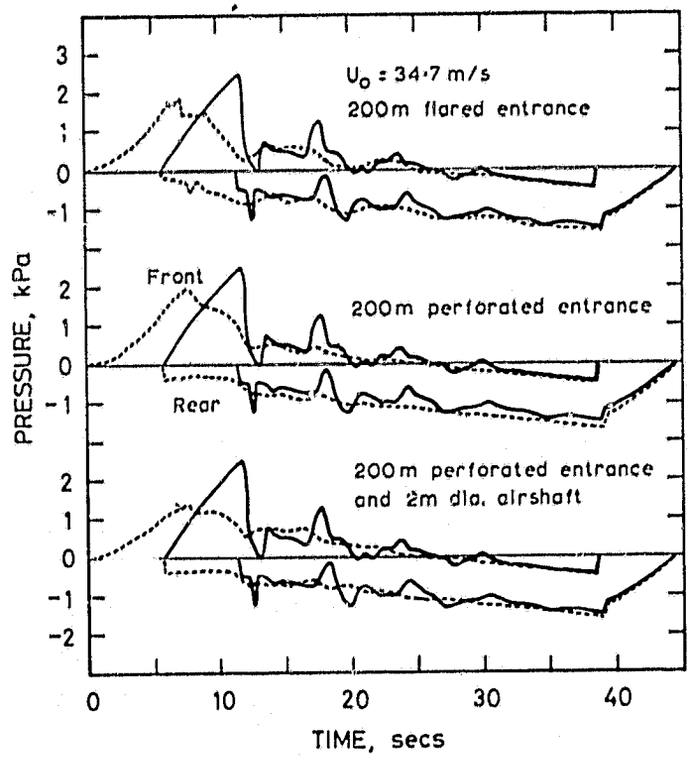

Fig. 6 The influence of various tunnel modifications on the pressure histories experienced by passengers on a train in Patchway Tunnel.
(———— = unmodified tunnel, ---------- = modified tunnel).

APPENDIX

PAGE 36 INTENTIONALLY BLANK

APPENDIX A
VOLUME II
TABLE OF CONTENTS

PAGE 38 INTENTIONALLY BLANK

TABLE OF CONTENTS (CONT'D)

TABLE OF CONTENTS (CONT'D)

TABLE OF CONTENTS (CONT'D)

LIST OF ILLUSTRATIONS

LIST OF ILLUSTRATIONS (CONT'D)

LIST OF ILLUSTRATIONS

LIST OF TABLES

APPENDIX B
VOLUME III
TABLE OF CONTENTS